ROCKY MOUNTAIN JOURNAL OF MATHEMATICS
Vol. , No. , YEAR
https://doi.org/rmj.YEAR..PAGE

A NUMERICAL APPROACH BASED ON VIETA-FIBONACCI POLYNOMIALS TO SOLVE FRACTIONAL ORDER ADVECTION-REACTION DIFFUSION PROBLEM

RASHMI SHARMA AND RAJEEV

ABSTRACT. In this article, we attempt to provide the numerical solution for a non-linear reaction-advection diffusion equation with fractional-order space-time derivatives in a finite domain. In the proposed scheme, time fractional derivative in Caputo sense is approximated by using the non-standard finite difference method and the fractional space derivative is specifically approximated by using Vieta-Fibonacci polynomials. These approximations generate a system of ordinary differential equations which is converted into an equivalent system of algebraic equations by using collocation method. Finally, the obtained system of algebraic equations is solved to find the dependent variables (unknowns) of the considered problem. The stability and convergence related to the time discreatization of this approach are also discussed. In this study, the effectiveness and precision of the proposed scheme are analyzed with the help of examples, and it is observed that the proposed scheme is sufficiently accurate and efficient technique. Also, the effects of fractional-order derivatives on concentration profiles are discussed.

1. Introduction

Groundwater is one of the essential needs of the living species and the quality of groundwater directly affects the human's life. An undesirable change in the quality of groundwater due to human activities is called groundwater contamination/pollution. Generally, groundwater contains several minerals in limited quantity, and the amount of minerals ions in water is measured in terms of the total dissolved solids (TDS) concentration. Nowadays groundwaters are getting polluted (water with high TDS concentration) due to the presence of a high concentration of some trace elements such as Arsenic and chronic. Groundwater pollution have different sources such as, fertilizers, pesticides, road salt, industrial wastes, etc,. It is also observed that the surface water is transported to the groundwater via caverns and open fissures without passing through a filter. All these substances diffuse into the groundwater through the existing natural porous media. In the literature, the mathematical formulations of solute transport in groundwater was presented by Bear and Verruijt [1], Fried [2], Gomez-Aguilar et al. [3] etc,. The phenomenon of transferring various physical quantities, such as particles, energy, or other quantities, into a physical system due to diffusion and advection processes are governed by advection-diffusion equations. Concentration gradients cause diffusion in the soil column, and advection will also contribute to the flow of chemical species if bulk fluid motion is present. Determining the combined effect of diffusion and advection along with the reaction term on the solution profile is a challenging task. The reaction-advection-diffusion equations arise in a wide range of scientific disciplines, such as biology, industrial, aerospace sciences, astrophysics and environmental

2020 *Mathematics Subject Classification.* 33C47, 42A10, 65M70, 65N99, 65Z05.
Key words and phrases. Advection-reaction-diffusion equation, fractional derivative in the Caputo sense, Shifted Vieta-Fibonacci polynomials, Collocation technique, Approximation method.

problems. The application of reaction-advection-diffusion equations can also be seen in the prediction of weather, various chemical reactions, transport of water vapor in the Earth's atmosphere, the process of energy and mass transfer, etc,.

In the last decade, the differential equations with fractional order have been attracted by many researchers because these equations are widely used for describing a variety of phenomena in the various fields, for example, medical and biological sciences, geological science, diffusion processes, heat and mass transfer, etc,. A brief introduction of fractional calculus can be seen in [4], and some recent works related to fractional derivative can also be found in [5], [6], [7], [8], [9], [10], [11]. The notion of a variable-order differential operator is an improvement, and its applications are rapidly growing due to its potential for describing many practical problems in different fields, such as problems of porous media [12], thermoelasticity [13], petroleum engineering [14], and many more branches of engineering and science.

The fractional reaction-advection-diffusion equation derives from the classic reaction-advection-diffusion equations and can be more properly model complicated physical phenomena like anomalous diffusion and sub/super diffusion and have features of temporal heredity and spatial global dependence. Compared with integer-order model, the fractional-order reaction-advection-diffusion model has a benefits of more describing complex processes, like heat conduction, seepage, convection diffusion, viscoelasticity, anomalous diffusion, and turbulence compared to its integer-order equivalent.

The variable-order fractional reaction advection-diffusion equation (RADEs) have a stronger ability to describe the diffusion process as compare to the fractional-order RADEs. From the literature survey, it is found that the variable-order fractional differential operator has become promising approach for describing the non-local properties. In the literature of variable-order RADEs, several methematical models have been presented by many authors, for example Heydari et al. [15] presented a model of coupled non-linear RADEs with variable-order (VO) fractional Caputo-Fabrizio derivative. Zhuang et al. [16] presented advection-diffusion equation (ADEs) with VO fractional derivative and a non-linear source term. They discussed Euler's scheme to solve the problem with stability and convergency of that method. Chen et al. [17] discussed a model of transport dynamics that involves a multi-term space-time VO fractional ADEs and they presented its solution with implicit numerical scheme. Kheirkhah et al. [18] presented a class of mathematical models of subdiffusion equations with VO time-fractional derivative, and they discussed a numerical solution for the problem. Owolabi [19] modeled the space-time fractional reaction-diffusion equation with the Caputo and Riesz operators. Agarwal et al. [20] formulated a numerical method based on Vieta-Fibonacci operational matrices to present an approximate solution to integro-diiferential equations with fractional VO derivative. Some more papers related to variable-order fractional derivative can be seen in [21], [22], [23], [24], [25], [26], [27].

Since the exact solution of several variable-order fractional ARDEs is very tough to find so in the literature, many numerical methods have been proposed. Dai et al. [28] introduced a new approach based on Legendre polynomials to find the approximate solution of ARDEs with time VO fractional derivative. An efficient approximate scheme is developed by Hosseininia et al. [29] to solve 2D ARDEs. This scheme is based on radial basis function and Bernoulli polynomials in shifted form. Qu et al. [30] presented a neural network method to solve the space-time VO fractional ADEs including a non-linear source term. In order to solve the VO fractional RADEs, Sharma and Rajeev [26], [27] discussed an operational matrix method based on different polynomials.

Due to the physical relevance, there is a lot of scope for researchers to explore variable-order ARDEs. In the present article, the authors consider the following VO time-space ARDEs in the Caputo sense:

$$\begin{aligned} {}_0^C D_\rho^{\alpha(w,\rho)} \zeta(w,\rho) =& \vartheta(\zeta,w,\rho) {}_0^C D_w^{1+\beta(w,\rho)} \zeta(w,\rho) - \delta(\zeta,w,\rho) {}_0^C D_w^{\gamma(w,\rho)} \zeta(w,\rho) \\ &+ \lambda\zeta(\zeta-1)(1-\zeta) + f(w,\rho), \end{aligned} \tag{1}$$

$$0 < \alpha(w,\rho) \le 1,\ 0 < \beta(w,\rho) \le 1,\ 0 < \gamma(w,\rho) \le 1,$$

with the following conditions:

$$\begin{aligned} \zeta(w,0) &= g_1(w), \\ \zeta(0,\rho) &= g_2(\rho), \\ \zeta(1,\rho) &= g_3(\rho), \end{aligned} \tag{2}$$

where $0 \le \rho \le 1$, $0 \le w \le 1$, $\alpha(w,\rho)$ and $\beta(w,\rho)$ are respectively time and space VO fractional derivatives in the Caputo sense, $\gamma(w,\rho)$ is the space fractional order derivative, $f(w,\rho)$ is the forced term. The solute concentration is denoted by $\zeta(w,\rho)$, the initial solute concentration is denoted by $g_1(w)$, $g_2(\rho)$ and $g_3(\rho)$ are describe the concentration at boundary points. In the reaction term, if λ=0, then the system is called conservative otherwise non-conservative. In the present model, we have consider the nonlinear diffusion and advection terms with nonlinear reaction term. From [31], it is clear that the nonlinear diffusive term increases the solute concentration in comparison to the linear diffusion case. In this study, our aim is to discuss the effect of nonlinear diffusion and advection terms on the solute transportations in the fluid flow of porous media. The physical phenomena like fast diffusion or slow diffusion is very much relevant for the porous media, and thus, the presence of nonlinear term plays an important role from the physical point of view as compared to a linear model. This has motivated the authors to solve a such type of porous media problem.

Here is a summary of the paper's organization. In section 2 we define an important tools and characteristics of the shifted Vieta-Fibonacci polynomials (SVFPs) to aid in the development of our proposed scheme. Section 3 discuss about approximation of an arbitrary function and the operational matrices for the takenpolynomials. Section 4 presents a brief overview of the developed scheme. Section 5 conclude about discussion of error analysis. Section 6 describes the numerical computations of the study, and the conclusion is presented in section 7.

2. Preliminary

This section provides some important definitions and properties of the SVFPs which are needed in the remaining part ot the article.

2.1. *Basic Definitions.* Assume a continuous function $\xi : [0,1] \times [0,T] \longrightarrow (q-1,q]$. For any arbitrary function $\nu(w,\rho)$, the VO fractional temporal partial differentiation of order $\xi(w,\rho)$ in the Caputo sense ([21], [22]) is given by

$$
(3) \quad {}_0^C D_\rho^{\xi(w,\rho)} v(w,\rho) = \begin{cases} \dfrac{1}{\Gamma(q-\xi(w,\rho))} \displaystyle\int_0^\rho (\rho-\eta)^{q-(\xi(w,\rho)+1)} \frac{\partial^q v(w,\eta)}{\partial \eta^q} d\eta, & q-1<\xi(w,\rho)\le q \\ \dfrac{\partial^q v(w,\rho)}{\partial \rho^q}, & \xi(w,\rho)=q\in\mathbb{N}. \end{cases}
$$

2.2. ***SVFPs.*** The well-known Vieta-Fibonacci polynomials are defined on the interval [-2,2] and satisfy the following recurrence relation

$$\mathrm{VF}_k(w) = y\mathrm{VF}_{k-1}(w) - \mathrm{VF}_{k-2}(w),\ k=2,3,...,$$

where

$$\mathrm{VF}_0(w)=0,\ \mathrm{VF}_1(w)=1.$$

The weight function $\sqrt{4-w^2}$ and the Vieta-Fibonacci polynomials $\mathrm{VF}_k(w)$ are orthogonal on [-2,2] in the following way:

$$\langle \mathrm{VF}_{k1}(w), \mathrm{VF}_{k2}(w)\rangle \quad = \int_{-2}^{2} \sqrt{4-w^2}\mathrm{VF}_{k1}(w)\mathrm{VF}_{k2}(w)dw \quad = \begin{cases} 0,\ k1\neq k2, \\ 2\pi,\ k1=k2. \end{cases}$$

To use Vieta-Fibonacci polynomials on the interval [0,1], let us define the SVFPs by taking w=$4w-2$. Let the SVFPs $\mathrm{VF}_i(4w-2)$ be denoted by $\mathrm{VF}_i^*(w)$. Then $\mathrm{VF}_i^*(w)$ can be obtained as follows:

$$\mathrm{VF}_k^*(w) = (4w-2)\mathrm{VF}_{k-1}^*(w) - \mathrm{VF}_{k-2}^*(w),\ k=2,3,...,$$

where $\mathrm{VF}_0^*(w)$=0 and $\mathrm{VF}_1^*(w)$=1. The analytic form of the SVFPs $\mathrm{VF}_i^*(w)$ is given below:

$$(4) \quad \mathrm{VF}_k^*(w) = \sum_{i=0}^{k} (-1)^i \frac{2^{2k-2i-2}\Gamma(2k-i)}{\Gamma(i+1)\Gamma(2k-2i)} w^{k-i-1},\ k\in\mathbb{Z}^+$$

or

$$(5) \quad \mathrm{VF}_k^*(w) = \sum_{i=0}^{k} (-1)^{k-i-1} \frac{2^{2i}\Gamma(k+i+1)}{\Gamma(k-i)\Gamma(2i+2)} w^{i},\ k\in\mathbb{Z}^+$$

By considering the weight function $\chi(w)=\sqrt{w-w^2}$ the polynomials $\mathrm{VF}_k^*(w)$ are orthogonal in the following manner:

$$
\begin{aligned}
\langle \mathrm{VF}_{k1}^*(w), \mathrm{VF}_{k2}^*(w)\rangle &= \int_0^1 \sqrt{w-w^2}\mathrm{VF}_{k1}^*(w)\mathrm{VF}_{k2}^*(w)dw, \\
(6) \quad &= \begin{cases} 0, & k1\neq k2, \\ \dfrac{\pi}{8}, & k1=k2\neq 0. \end{cases}
\end{aligned}
$$

3. Aproximation of an Arbitrary Function

Suppose $\ell(\rho) = \left[\mathrm{VF}_1^*(\rho), ..., \mathrm{VF}_{(k+1)}^*(\rho)\right]^T \in L^2[0,1]$ is the set of SVFPs. Then a function $\zeta(\rho) \in L^2[0,1]$ can be written in terms of SVFPs as:

$$\zeta(\rho) = \sum_{i=1}^{\infty} c_i \mathrm{VF}_i^*(\rho), \tag{7}$$

the following formula is used to determine the coefficients c_i as follow

$$c_i = \frac{8}{\pi} \int_0^1 \zeta(\rho) \mathrm{VF}_i^*(\rho) \chi(\rho) d\rho. \tag{8}$$

An endeavour can truncate the above series as follows:

$$\zeta_k(\rho) \simeq \sum_{i=1}^{n+1} c_i \mathrm{VF}_i^*(\rho) = C^T \ell(\rho), \tag{9}$$

where notation T means transposition and

$$C = [c_1, c_2, ..., c_{k+1}]^T, \tag{10}$$

$$\ell(\rho) = \left[\mathrm{VF}_1^*(\rho), \mathrm{VF}_2^*(\rho), ..., \mathrm{VF}_{k+1}^*(\rho)\right]^T. \tag{11}$$

Similiarly, an arbitrary function $\zeta(w,\rho) \in L^2[0,1] \times L^2[0,1]$ can be written in terms of SVFPs as:

$$\zeta_k(w,\rho) \simeq \sum_{i=1}^{k+1} \sum_{j=1}^{k+1} c_{ij} \mathrm{VF}_i^*(w) \mathrm{VF}_j^*(\rho) = \ell^T(w) \mathrm{C} \ell(\rho), \tag{12}$$

where the entries of the matrix C=[c_{ij}] can be calculated as

$$c_{ij} = \frac{64}{\pi^2} \int_0^1 \int_0^1 \zeta(w,\rho) \mathrm{VF}_i^*(w) \mathrm{VF}_j^*(\rho) \chi(w) \chi(\rho) dw d\rho. \tag{13}$$

The definition of the first-order derivative for shifted Vieta-Fibonacci vector $\ell(\rho)$ is given as:

$$\frac{d\ell(\rho)}{d\rho} = \mathbf{D}\ell(\rho) \tag{14}$$

where $\ell(.)$ is defined in Eq. (11) and $\mathbf{D}$ is the $(k+1)\times(k+1)$ operational matrix of the shifted Vieta-Fibonacci vector $\ell(\rho)$ for first-order derivative with the following entries:

$$\mathbf{D} = \begin{cases} 4j, & i = 2,3,...(k+1),\ j = 1,2,...,i-1,\ i+j \text{ is odd}, \\ 0, & \text{otherwise}. \end{cases} \tag{15}$$

3.1. *The Operational Matrix for Fractional Differentiation.*

Lemma 1. *Let* $\mathrm{VF}_i^*(w)$ *be a SVFPs then*

$$ {}_0^C D_w^{\xi(w,\rho)} \mathrm{VF}_i^*(w) = 0,\ i = 1,\dots,p-1,\ p-1 < \mu(w,\rho) \le p,\ p \in \mathbb{N}. \tag{16}$$

In the following theorem, we generalise the operational matrix of SVFPs for fractional derivative of variable order.

Theorem 2. *Let* $\ell(w)$ *be shifted Vieta-Fibonacci vector defined as Eq.* (11) *and also suppose* $\xi(w,\rho) > 0$ *then*

$$ {}_0^C D_w^{\xi(w,\rho)} \ell(w) = \Psi_w^{\xi(w,\rho)} \ell(w), \tag{17}$$

where $\Psi_w^{\xi(w,\rho)}$ *is the operational matrix of order* $(k+1)\times(k+1)$ *for fractional differentiation of variable order* $\xi(w,\rho)$*, which is described as below:*

$$ \Psi_w^{\xi(w,\rho)} = w^{-\xi(w,\rho)} \begin{pmatrix} 0 & 0 & \cdots & 0 \\ \vdots & \vdots & \cdots & \vdots \\ 0 & 0 & \cdots & 0 \\ \sum_{i=p}^{p} \Pi_{p,z,i,1}^{\xi(w,\rho)} & \sum_{i=p}^{p} \Pi_{p,z,i,2}^{\xi(w,\rho)} & \cdots & \sum_{i=p}^{p} \Pi_{p,z,i,k+1}^{\xi(w,\rho)} \\ \vdots & \vdots & \cdots & \vdots \\ \sum_{i=p}^{k} \Pi_{k,z,i,1}^{\xi(w,\rho)} & \sum_{i=p}^{k} \Pi_{k,z,i,2}^{\xi(w,\rho)} & \cdots & \sum_{i=p}^{k} \Pi_{k,z,i,k+1}^{\xi(w,\rho)} \\ \vdots & \vdots & \cdots & \vdots \\ \sum_{i=p}^{k+1} \Pi_{k+1,z,i,1}^{\xi(w,\rho)} & \sum_{i=p}^{k+1} \Pi_{k+1,z,i,2}^{\xi(w,\rho)} & \cdots & \sum_{i=p}^{k+1} \Pi_{k+1,z,i,k+1}^{\xi(w,\rho)} \end{pmatrix}, \tag{18}$$

where

$$ \Pi_{k,z,i.j}^{\xi(w,\rho)} = \frac{8}{\pi} \sum_{z=0}^{j} \frac{(-1)^{(k+j-z-i-2)} (2)^{2(z+i)} \Gamma(k+j+z+i+2) \Gamma(i+1)}{\Gamma(k-i)\Gamma(j-z)\Gamma(2z+2)\Gamma(2i+2)\Gamma(i+1-\xi(w,\rho))} \left(\frac{\sqrt{\pi}}{2} \frac{\Gamma(i+z+3/2)}{i+z+3} \right). \tag{19}$$

Proof. The proof is done in [26]. □

4. Discription of the Present Method

In this section we use operational matrix scheme which is based on SVFPs to find the approximate solution of following nonlinear variable-order fractional ARDEs:

$$ \begin{aligned} {}_0^C D_\rho^{\alpha(w,\rho)} \zeta(w,\rho) =& \vartheta(\zeta,w,\rho) {}_0^C D_w^{1+\beta(w,\rho)} \zeta(w,\rho) - \delta(\zeta,w,\rho) {}_0^C D_w^{\gamma(w,\rho)} \zeta(w,\rho) \\ & + \lambda \zeta(\zeta-1)(1-\zeta) + f(w,\rho), \end{aligned} \tag{20}$$

$$ 0 < \alpha(w,\rho) \le 1,\ 0 < \beta(w,\rho) \le 1,\ 0 < \gamma(w,\rho) \le 1. $$

with following conditions:

$$ \begin{aligned} \zeta(w,0) &= g_1(w), \\ \zeta(0,\rho) &= g_2(\rho), \\ \zeta(1,\rho) &= g_3(\rho). \end{aligned} \tag{21}$$

where $0 \le w \le 1$, $0 \le \rho \le 1$. We shall approximate $\zeta(w,\rho)$ by SVFPs as

$$\zeta_k(w,\rho) \simeq \sum_{i=1}^{k+1}\sum_{j=1}^{k+1} c_{ij}\mathrm{VF}_i^*(w)\mathrm{VF}_j^*(\rho), \tag{22}$$

where c_{ij} are the unknown coefficients for $i = 1,...,(k+1)$, and $j = 1,...,(k+1)$. Now, we write

$$\zeta_k(w,\rho) = (\ell(w))^T \mathrm{C}\ell(\rho), \tag{23}$$

where matrix $\mathrm{C} = [c_{ij}]_{(k+1)\times(k+1)}$ is of unknowns and $\ell(\rho) = [\mathrm{VF}_1^*(\rho), \mathrm{VF}_2^*(\rho),...,\mathrm{VF}_{k+1}^*(\rho)]^T$ is a column vector. Now, substituting

$$ {}_0^C D_\rho^{\alpha(w,\rho)}\zeta(w,\rho) = (\ell(w))^T.\mathrm{C}.({}_0^C D_\rho^{\alpha(w,\rho)}\ell(\rho)) = (\ell(w))^T.\mathrm{C}.(\Psi_\rho^{\alpha(w,\rho)}\ell(\rho)), \tag{24}$$

$$ {}_0^C D_w^{\gamma(w,\rho)}\zeta(w,\rho) = ({}_0^C D_w^{\gamma(w,\rho)}\ell(w))^T.\mathrm{C}.\ell(\rho) = (\Psi_w^{\gamma(w,\rho)}\ell(w))^T.\mathrm{C}.\ell(\rho), \tag{25}$$

$$ {}_0^C D_w^{1+\beta(w,\rho)}\zeta(w,\rho) = ({}_0^C D_w^{1+\beta(w,\rho)}\ell(w))^T.\mathrm{C}.\ell(\rho) = (\Psi_w^{1+\beta(w,\rho)}\ell(w))^T.\mathrm{C}.\ell(\rho), \tag{26}$$

in the Eq.(20), we get

$$\begin{aligned}(\ell(w))^T.\mathrm{C}.(\Psi_\rho^{\alpha(w,\rho)}\ell(\rho)) =& \vartheta(((\ell(w))^T.\mathrm{C}.\ell(\rho)),w,\rho).(\Psi_w^{1+\beta(w,\rho)}\ell(w))^T.\mathrm{C}.\ell(\rho)\\ &-\delta(((\ell(w))^T.\mathrm{C}.\ell(\rho)),w,\rho).(\Psi_w^{\gamma(w,\rho)}\ell(w))^T.\mathrm{C}.\ell(\rho)\\ &+\lambda(((\ell(w))^T.\mathrm{C}.\ell(\rho)).((\ell(w))^T.\mathrm{C}.\ell(\rho)-1).(1-(\ell(w))^T.\mathrm{C}.\ell(\rho))\\ &+f(w,\rho).\end{aligned} \tag{27}$$

from the conditions (2) and the Eq. (23), we get

$$(\ell(w))^T\mathrm{C}\ell(0) = g_1(w),\ (\ell(0))^T\mathrm{C}\ell(\rho) = g_2(\rho),\ (\ell(1))^T\mathrm{C}\ell(\rho) = g_3(\rho). \tag{28}$$

Now, we collocate Eq. (27) with the aid of Eq. (28) at points $w_i = \frac{i}{k}$ for i=1,2,..,N and $\rho_i = \frac{i}{k}$ where $i = 1,2,...,k$. A set of nonlinear algebraic equations is generated in this stage which yields the solution for coefficients of the matrix C. Using this method, we can obtain the numerical solution for our suggested VO fractional ARDEs, (1)(2).

5. Convergence and Error Analysis

Theorem 3. *Assume that $\zeta_k(w,\rho)$ be the approximation of $\zeta(w,\rho)$ in the terms of shifted Vieta-Fibonacci polynomials. If the function $\zeta(w,\rho)$ has continuous bounded derivatives of fourth partial order, i.e. $\zeta_k^{''''}(w,\rho) \le K$, then the numerical solution series $\zeta_k(w,\rho)$ converges uniformly to the function $\zeta(w,\rho)$. In addition, the coefficients υ_{ij} is bounded, i.e.*

$$|\upsilon_{ij}| \le \frac{K}{4(i-2)^2(j-2)^2}\ i>2, j>2.$$

Proof. The proof of this theorem is given in [10], and one can conclude that the series $\sum_{i=1}^{\infty}\sum_{j=1}^{\infty}\upsilon_{ij}$ is absolutely and uniformly convergent and hence the approximate solution series uniform converges to the function $\zeta(w,\rho)$. □

Theorem 4. *Assume that the approximate solution $\zeta_k(w,\rho)$ is the best approximation to the $\zeta(w,\rho)$ as stated in Eq. (12). Suppose that the function $\zeta(w,\rho)$ is continuously differentiable k times on [0,1] and M is any number such that for all w' between 0 and 1 and all ρ' between 0 and 1,*

$$\left|\sum_{i=0}^{k+1}\frac{\partial^{k+1}}{\partial w^i\partial\rho^{k+1-i}}\zeta(w',\rho')\right|\leq M,$$

then

$$||\zeta(w,\rho)-\zeta_k(w,\rho)||_{L^2}\leq\begin{cases}M\left|\dfrac{(k+2)}{\frac{k+1}{2}!\frac{k+1}{2}!}\right|\dfrac{\pi}{8}, & k=odd,\\ M\left|\dfrac{(k+2)}{\frac{k}{2}!\frac{k+1}{2}!}\right|\dfrac{\pi}{8}, & k=even.\end{cases}\tag{29}$$

Proof. By using Taylor's theorem, expanding $\zeta(w,\rho)$ about the point (w_0,ρ_0), we get

$$\begin{aligned}\zeta(w,\rho)=&\zeta(w_0,\rho_0)+\zeta_w(w_0,\rho_0)(w-w_0)+\zeta_\rho(w_0,\rho_0)(\rho-\rho_0)+\frac{\zeta_{ww}(w_0,\rho_0)}{2}(w-w_0)^2\\&+\zeta_{w\rho}(w_0,\rho_0)(w-w_0)(\rho-\rho_0)+\frac{\zeta_{\rho\rho}(w_0,\rho_0)}{2}(\rho-\rho_0)^2+\ldots\\&+\sum_{i=0}^{k+1}\sum_{j=0}^{k+1-i}\frac{\frac{d^{(i+j)}\zeta}{\partial w^i\partial\rho^j}(\kappa,\theta)}{i!j!}(w-\kappa)^i(\rho-\theta)^j+\frac{\frac{\partial^{k+1}}{\partial w^{k+1}}\zeta(\kappa,\theta)}{k+1!}(w-w_0)^{k+1}\\&+\frac{\frac{\partial^k}{\partial w^k}\frac{\partial}{\partial\rho}\zeta(\kappa,\theta)}{k!1!}(w-w_0)^k(\rho-\rho_0)+\frac{\frac{\partial^{k-1}}{\partial w^{k-1}}\frac{\partial^2}{\partial\rho^2}\zeta(\kappa,\theta)}{(k-1)!2!}(w-w_0)^{(k-1)}(\rho-\rho_0)^2+\ldots\\&+\frac{\frac{\partial^{k+1}}{\partial\rho^{k+1}}\zeta(\kappa,\theta)}{k+1!}(\rho-\rho_0)^{k+1},\end{aligned}\tag{30}$$

where the point $(w_0,\rho_0)\in[0,1]\times[0,1]$ and $(\kappa,\theta)\in(w_0,w)\times(\rho_0,\rho)$. Suppose $k+1$ terms of the series (37) is the approximation $(\tilde{\zeta}_k(w,\rho))$ of $\zeta(w,\rho)$, i.e.

$$\tilde{\zeta}_k(w,\rho)=\sum_{r=0}^{k}\sum_{s=0}^{k-r}\frac{\frac{\partial^r}{\partial w^r}\frac{\partial^s}{\partial\rho^s}\zeta(w_0,\rho_0)}{r!s!}(w-w_0)^r(\rho-\rho_0)^s,\tag{31}$$

then the absolute error is defined as follows:

$$\begin{aligned}&||\zeta(w,\rho)-\tilde{\zeta}_k(w,\rho)||\\&=\left|\frac{\frac{\partial^{k+1}}{\partial w^{k+1}}\zeta(\kappa,\theta)}{k+1!}(w-w_0)^{k+1}+\frac{\frac{\partial^k}{\partial w^k}\frac{\partial}{\partial\rho}\zeta(\kappa,\theta)}{k!1!}(w-w_0)^k(\rho-\rho_0)+\ldots+\frac{\frac{\partial^{k+1}}{\partial\rho^{k+1}}\zeta(\kappa,\theta)}{k+1!}(\rho-\rho_0)^{k+1}\right|.\end{aligned}$$

Since, $\zeta_k(w,\rho)$, is the best square approximation of $\zeta(w,\rho)$, then the following inequality holds:

$$||\zeta(w,\rho)-\zeta_k(w,\rho)||^2 \leq ||\zeta(w,\rho)-\tilde{\zeta}_k(w,\rho)||^2$$
$$= \int_0^1\int_0^1 \chi(w)\chi(\rho)\left[\zeta(w,\rho)-\tilde{\zeta}_k(w,\rho)\right]^2 dwd\rho,$$

where $\chi(w)=\sqrt{w-w^2}$ and $\chi(\rho)=\sqrt{\rho-\rho^2}$.

After some mathematical calculations, we get

$$||\zeta(w,\rho)-\zeta_k(w,\rho)||^2 \leq \begin{cases} M^2\left|\dfrac{(k+2)}{\frac{k+1}{2}!\frac{k+1}{2}!}\right|^2\displaystyle\int_0^1\int_0^1\chi(w)\chi(\rho)dwd\rho, & k=\text{odd},\\ M^2\left|\dfrac{(k+2)}{\frac{k}{2}!\frac{k}{2}!}\right|^2\displaystyle\int_0^1\int_0^1\chi(w)\chi(\rho)dwd\rho, & k=\text{even}.\end{cases} \tag{32}$$

Then Eq. (32) can be rewritten as:

$$||\zeta(w,\rho)-\zeta_k(w,\rho)||^2 \leq \begin{cases} M^2\left|\dfrac{(k+2)}{\frac{k+1}{2}!\frac{k+1}{2}!}\right|^2\dfrac{\pi^2}{64}, & k=\text{odd},\\ M^2\left|\dfrac{(k+2)}{\frac{k}{2}!\frac{k}{2}!}\right|^2\dfrac{\pi^2}{64}, & k=\text{even}.\end{cases} \tag{33}$$

After some mathematical manipulation to the square root of Eq.(34), we achive an upper bound and subsequently $||\zeta(w,\rho)-\zeta_k(w,\rho)|| \to 0$ tends to zero with the order of $O\left(\frac{1}{k}\right)$ when $k\to\infty$, which establishes that the approximate solution becomes nearly equal to the exact solution if k is high enough. The proof is finished. □

6. Numerical Experiments

Now, we take the following two examples to show the accuracy of the suggested approach:

Example 6.1. Let us consider the following VO time fractional diffusion equation [23]:

$$\frac{\partial^{\alpha(w,\rho)}\zeta(w,\rho)}{\partial\rho^{\alpha(w,\rho)}} = \frac{\partial^2\zeta(w,\rho)}{\partial w^2} + f(w,\rho), \tag{34}$$

with initial and boundary conditions

$$\zeta(w,0)=0,\ w\in[0,1], \tag{35}$$
$$\zeta(0,\rho)=\rho^{\rho},\ \zeta(1,\rho)=\rho^{\rho}e,\ t\in[0,1], \tag{36}$$

where $f(w,\rho)=\rho^{\rho}e^{w}\left(\frac{\Gamma(\rho+1)}{\Gamma(\rho+1-\alpha(w,\rho))}\rho^{-\alpha(w,\rho)}-1\right)$, $\rho\in\mathbf{R}^+$.

As given by [24], [25], we define experimental convergence order (ECO) as

$$\text{ECO} = \frac{log\left(\frac{R_{k_1}(\rho)}{R_{k_2}(\rho)}\right)}{log\left(\frac{k_2}{k_1}\right)}, \tag{37}$$

where $R_{k_1}(\rho)$ and $R_{k_2}(\rho)$ are the maximum absolute error arisen in the k_1 and k_2 simulations at time ρ.

The exact solution of the problem (34)-(36) is $\zeta(w,\rho) = \rho^{\rho} e^{w}$. This problem has been solved by accurate discretization technique [23] for different derivative orders $\alpha(w,\rho)$ and ρ=5. The L_∞ errors of obtained approximated solution by proposed method are compared with results of [23] and these errors are depicted in Table (1). From this table, it is clear that the accuracy of our proposed approach is better than the technique discussed by Hajipour et al. [23]. Table (2) demonstrates the effect of k on the convergence of the solutions. It can be realised that by increasing the degree of SVFPs (k), the solutions converge with higher precision. It is evident that ECO≈1 with respect to k. It is notice from the table that as the value of k increases, the maximum absolute error (MAE) reduces and eventually the solutions converges to exact value. Table (1) and (2) confirm that the solution is convergent with high accuracy and an acceptable convergence rate that demonstrates the validity and usefulness of our proposed numerical approach.

TABLE 1. Comparison of L_∞ error for different functions with asending order of polynomial degree k.

$\alpha(w,\rho)$	k	error [23]	k	proposed MAE
$\frac{e^{-w}}{300}$	4	3.0923×10^{-6}	3	4.3527×10^{-9}
	8	1.9362×10^{-7}	5	8.7953×10^{-10}
	16	1.2190×10^{-8}	8	3.5663×10^{-11}
	32	7.6231×10^{-10}	11	2.0175×10^{-12}
	64	4.7680×10^{-11}	15	2.9906×10^{-13}
$\frac{2w+1}{300}$	4	3.0899×10^{-6}	3	4.3457×10^{-9}
	8	1.9347×10^{-7}	5	8.7562×10^{-10}
	16	1.2181×10^{-8}	8	3.5659×10^{-11}
	32	7.6171×10^{-10}	11	1.9968×10^{-12}
	64	4.7645×10^{-11}	15	2.9857×10^{-13}
$\frac{20e^{\frac{w}{2}}-12}{20e^{\frac{w}{2}}-10}$	4	2.8766×10^{-6}	3	3.9785×10^{-9}
	8	1.8012×10^{-7}	5	7.1658×10^{-10}
	16	1.1242×10^{-8}	8	3.1589×10^{-11}
	32	7.0088×10^{-10}	11	1.2382×10^{-12}
	64	4.3802×10^{-11}	15	1.1253×10^{-13}

TABLE 2. Table of maximum absolute error and ECO for example 6.1.

k	11	12	13	14	15
MAE	1.091425×10^{-12}	6.18592×10^{-13}	3.98012×10^{-13}	2.77169×10^{-13}	2.03905×10^{-13}
ECO	-	0.98684	0.98807	0.99235	0.99569

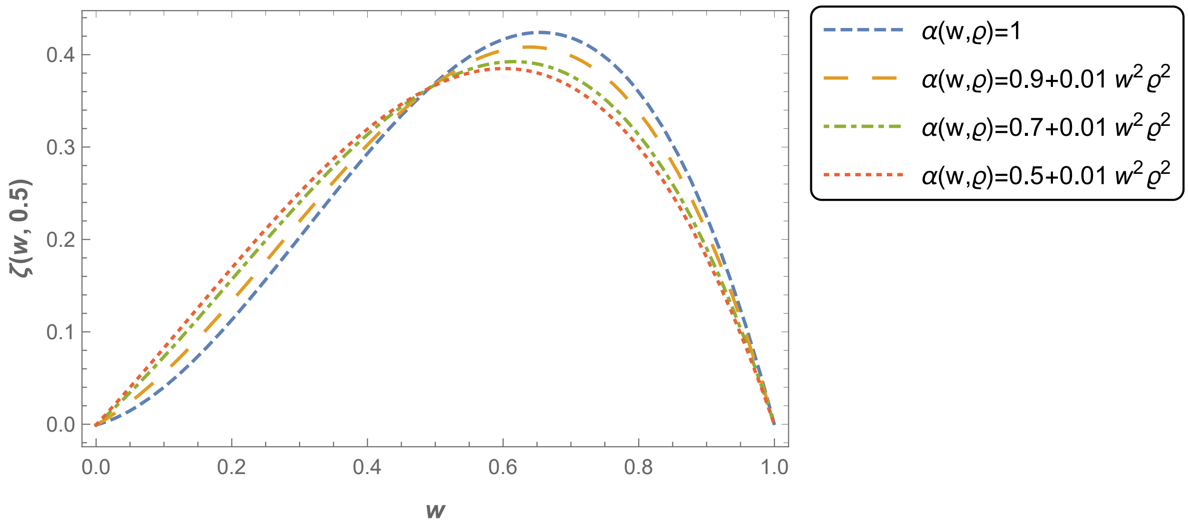

FIGURE 1. Plot of solute concentration $\zeta(w,\rho)$ vs. w for nonconservative system when $\alpha(w,\rho) = x + 0.01w^2\rho^2$.

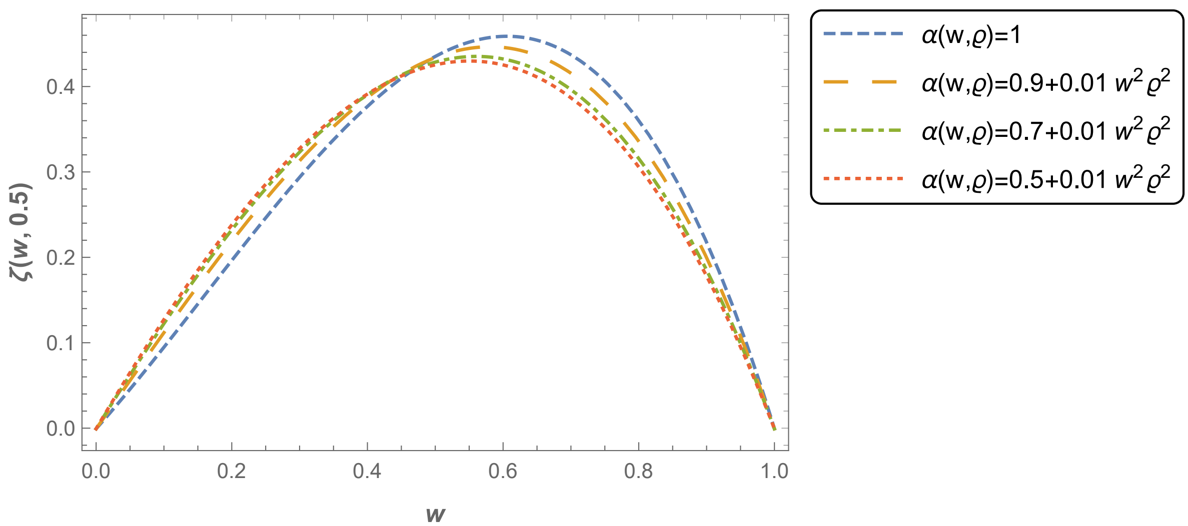

FIGURE 2. Plot of solute concentration $\zeta(w,\rho)$ vs. w for conservative system when $\alpha(w,\rho) = x + 0.01w^2\rho^2$.

Example 6.2. Let us take $\vartheta(w,\rho) = \frac{-\Gamma(2.6)w^{0.4}\rho^{1.4}}{\Gamma(2.4)}$, $\delta(\zeta,w,\rho) = \frac{-5\Gamma(1.4)w^{1.6}\rho^{1.4}}{\Gamma(2.4)}$ and λ=0 then we have the following non-linear fractional-order ADE :

$$
\begin{aligned}
D_\rho^{\alpha(w,\rho)}\zeta(w,\rho) =& \frac{-\Gamma(2.6)w^{0.4}\rho^{1.4}}{\Gamma(2.4)} D_w^{1+\beta(w,\rho)}\zeta(w,\rho) \\
&+ \frac{5\Gamma(1.4)w^{1.6}\rho^{1.4}}{\Gamma(2.4)} D_w^{\gamma(w,\rho)}\zeta(w,\rho) + f(w,\rho),
\end{aligned}
\tag{38}
$$

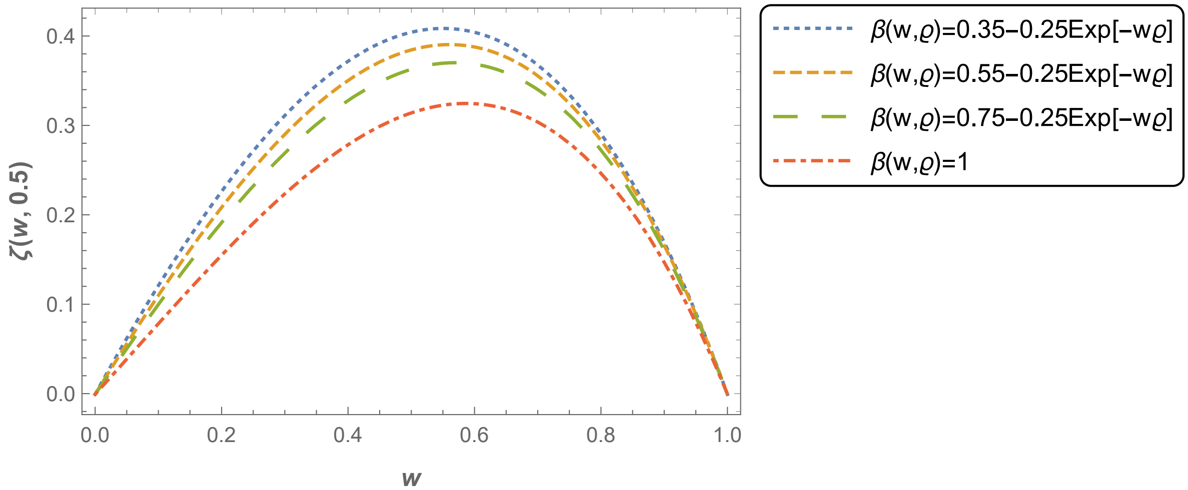

FIGURE 3. Plot of solute concentration $\zeta(w,\rho)$ vs. w for nonconservative system when $\beta(w,\rho) = x - 0.25exp[-w\rho]$.

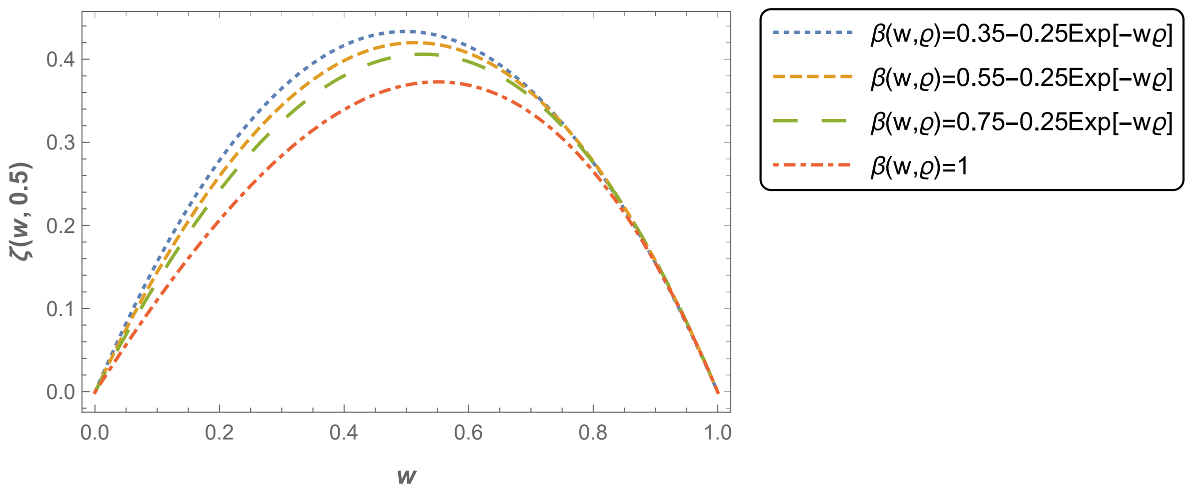

FIGURE 4. Plot of solute concentration $\zeta(w,\rho)$ vs. w for conservative system when $\beta(w,\rho) = x - 0.25exp[-w\rho]$.

subject to the given conditions:

$$\zeta(w,0) = w^2,\ 0 \le w \le 1, \tag{39}$$

$$\zeta(0,\rho) = 0, \tag{40}$$

$$\zeta(1,\rho) = 1 + 4\rho^2, \tag{41}$$

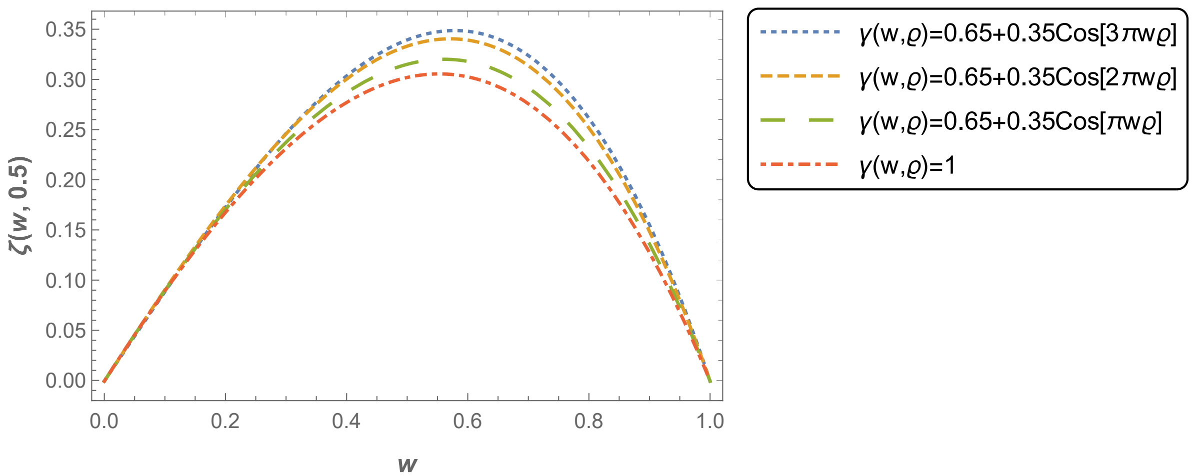

FIGURE 5. Plot of solute concentration $\zeta(w,\rho)$ vs. w for nonconservative system when $\gamma(w,\rho) = 0.65 - 0.35\cos[xw\rho]$.

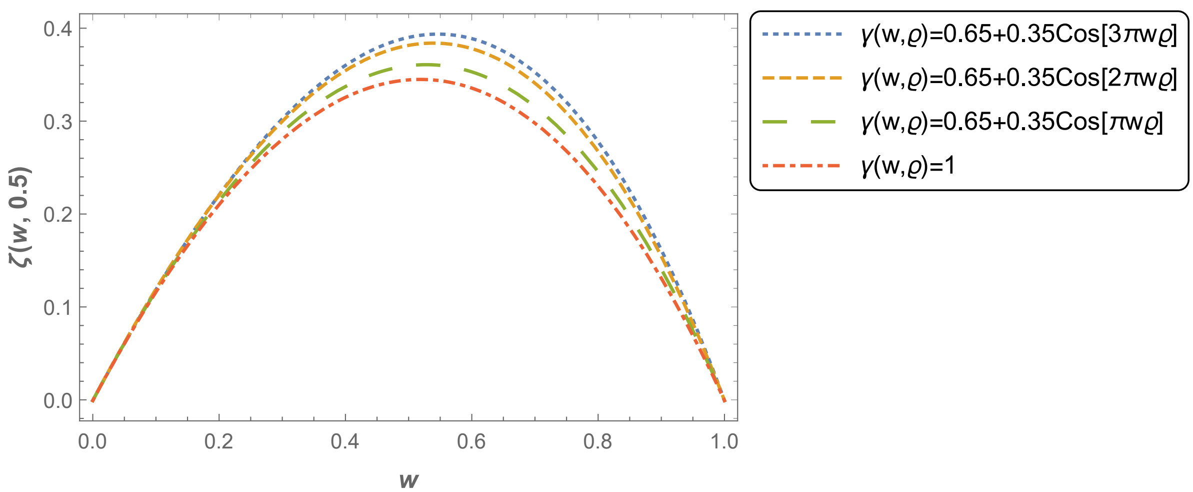

FIGURE 6. Plot of solute concentration $\zeta(w,\rho)$ vs. w for conservative system when $\gamma(w,\rho) = 0.65 - 0.35\cos[xw\rho]$.

where

$$\alpha(w,\rho) = 0.6,\ \beta(w,\rho) = 1.6,\ \gamma(w,\rho) = 0.6,\ f(w,\rho) = \frac{-32\,w^2\rho^{3.4}}{\Gamma(2.4)}.$$

The exact solution to the problem (38)-(41) is given by,

$$\zeta(w,\rho) = (1+4\rho^2)w^2. \tag{42}$$

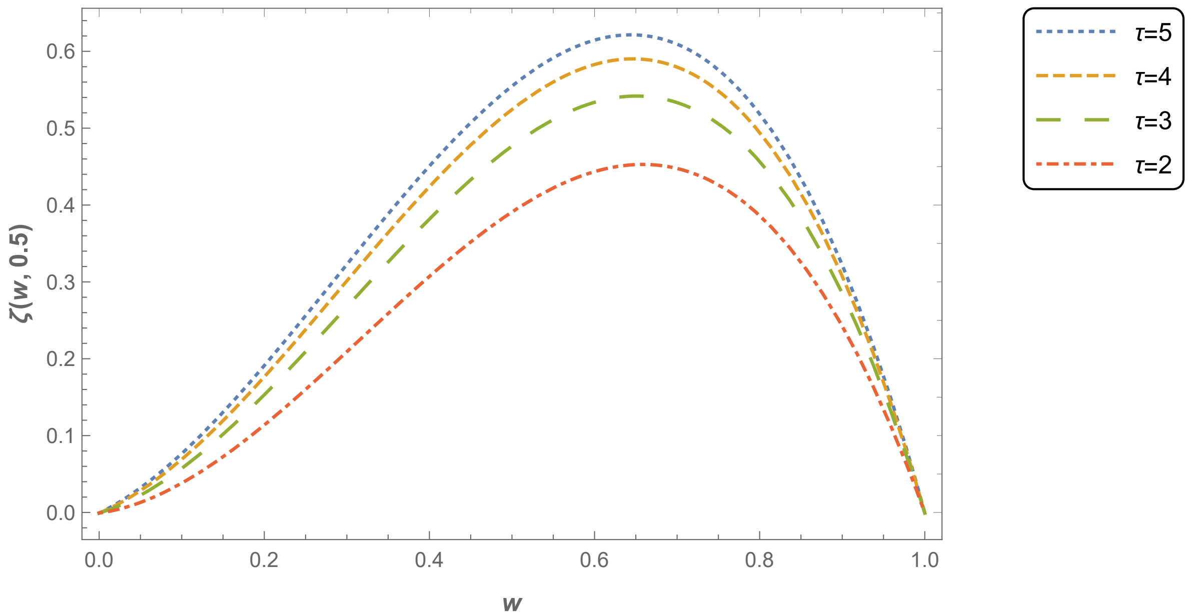

FIGURE 7. Plot of solute concentration $\zeta(w,\rho)$ vs. w for nonconservative system at various value of τ.

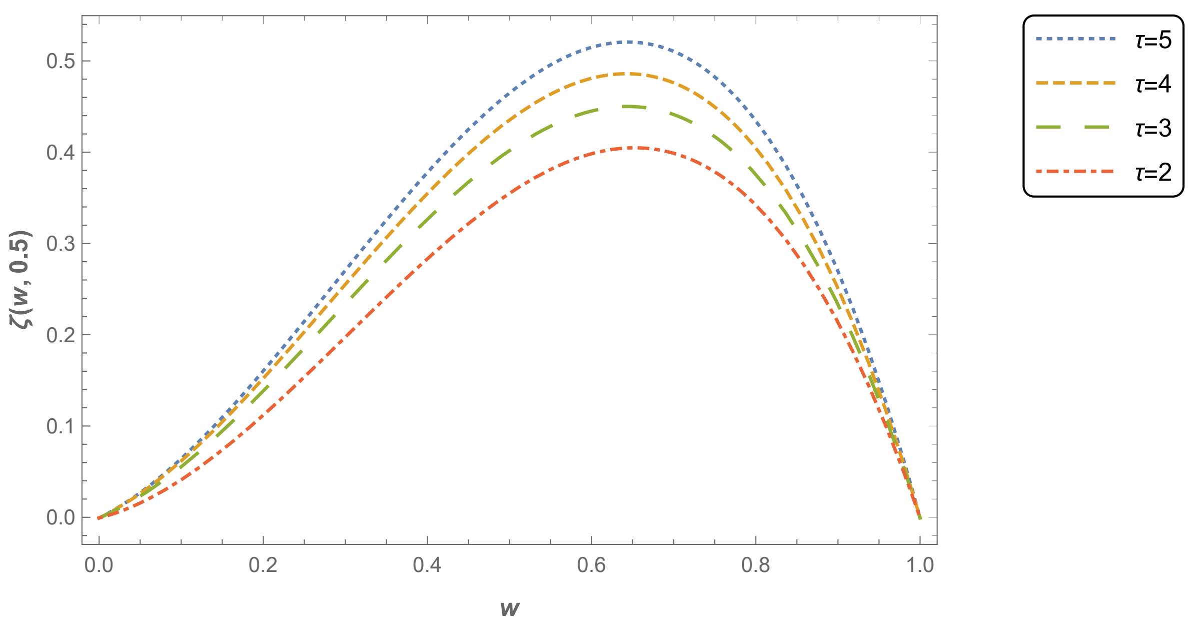

FIGURE 8. Plot of solute concentration $\zeta(w,\rho)$ vs. w for conservative system at various value of τ.

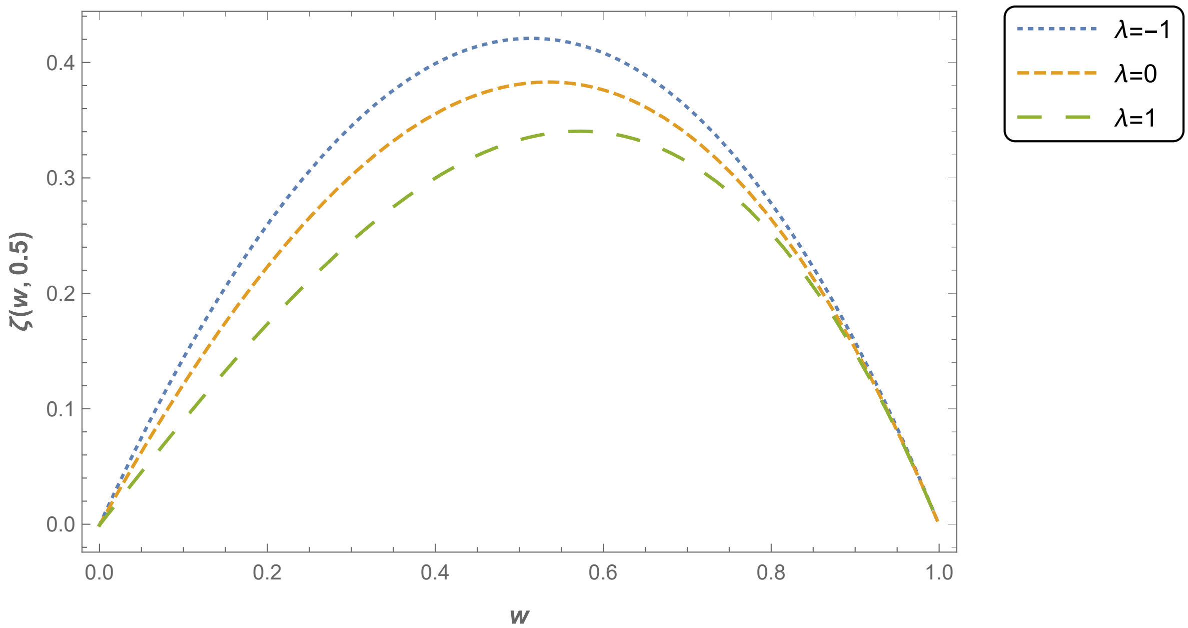

FIGURE 9. Plot of solute concentration $\zeta(w,\rho)$ vs. w at different value of λ.

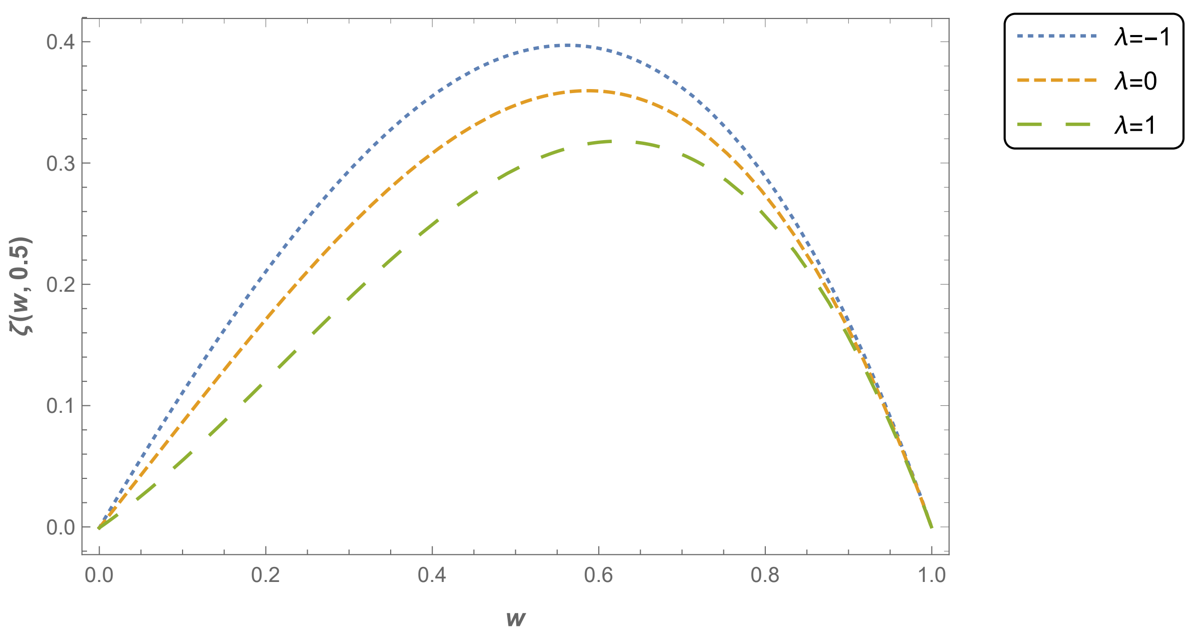

FIGURE 10. Plot of solute concentration $\zeta(w,\rho)$ vs. w at different value of λ.

A comparison of absolute errors obtained by proposed technique and Liu et al.,[11] is shown in Table (3). Table (3) clearly depicts that the accuracy of our proposed scheme is higher as compared to the numerical method proposed by Liu et al.,[11] .

TABLE 3. Comparison of absolute errors for our proposed method and the method given in Liu et al.,[11].

w	Proposed Method	IDM [11]
0.2	2.132×10^{-4}	3.948×10^{-2}
0.4	9.787×10^{-5}	1.990×10^{-2}
0.6	5.156×10^{-4}	7.940×10^{-3}
0.8	6.223×10^{-4}	3.941×10^{-3}

After the validation of precision and effectiveness of our numerical method, an endeavor has been taken to find the solution of the considered nonlinear space-time variable-order ARDEs (1) to exhibit the behaviour of solute concentration for conservative system (CS) and non-conservative system (NCS) under the following conditions:

$$\zeta(w,0) = w^2(1-w^2), \tag{43}$$

$$\zeta(0,\rho) = 0,\ \zeta(1,\rho) = 0. \tag{44}$$

Figs (1)-(10) are plotted to show the dependence of the solute concentration profiles on various parameters by using the proposed operational matrix along with the collocation approach for the variable-order ADREs (1) for $\rho = 0.5$, $f(w,\rho) = w - w\rho^2$, $\vartheta(\zeta,w,\rho) = \zeta^\tau$, $\delta(\zeta,w,\rho) = \zeta$. Figs. (1) and (2) show the concave downward solute concentration profiles for various polynomial functions of the type $\alpha(w,\rho) = x + 0.01w^2\rho^2$ in the case of NCS and CS respectively at the fixed value of $\beta(w,\rho) = 0.55 + 0.25\sin[\pi\rho]$ and $\gamma(w,\rho) = 0.55 - 0.25\cos[\rho]$. These figures depict the similar behavior of the solute concentration profiles for the non-conservative and conservative systems. In Figures (1) and (2), it is seen that the solute concentration profiles first increase to its maximum value then continuously decreses to 0 at the end point. Figs. (3) and (4) present the solute concentration profiles for different exponential functions $\beta(w,\rho) = x - 0.25exp[-w\rho]$ at $\alpha(w,\rho) = \frac{20-exp(w\rho)}{600}$, $\gamma(w,\rho) = \frac{2+\sin(w\rho)}{4}$ in the case of NCS and CS, respectively. Figs. (3)-(4) reveal that the solute concentration profiles grow as the value x increases for both the NCS and CS. Figs. (5) and (6) depict the effect of oscillatory function $\gamma(w,\rho) = 0.65 + 0.35\cos[xw\rho]$ on the solute concentration profiles at $\alpha(w,\rho) = 0.45 - 0.25exp[-w\rho]$, $\beta(w,\rho) = 0.65 + 0.25\sin[\pi w\rho]$ for the NCS and CS, respectively. These figures demonstrate that the diffusion becomes fast for the CS and NCS when the angle of the function $\gamma(w,\rho)$ grows. In Figs. (1)-(6), it is seen that the peaks of the solute concentration profiles are higher for CS than the NCS in all the cases, and diffusion is faster for CS than the NCS. Figs. (7) and (8) are plotted at $\alpha(w,\rho) = 0.55 + 0.45\sin[\pi\rho]$, $\beta(w,\rho) = \frac{15+\cos(w\rho)}{450}$, $\gamma(w,\rho) = 0.45 - 0.25exp[-w\rho]$ to demonstrate the effect of τ (nonlinearity in diffusion term) on the solute concentration profiles for the NCS and CS, respectively. It is seen from these figures that the diffusion process becomes fast for the CS and NCS as the value of τ grows. Figs. (9) and (10) are shown to present the effect of λ

on the diffusion process with the advection term and without advection term, respectively. Fig. (9) is plotted for $\alpha(w,\rho) = \frac{20-exp(w\rho)}{600}$, $\beta(w,\rho) = 0.8+0.01w^2\rho^2$, $\gamma(w,\rho) = 0.45+0.25\sin[2\rho]$ and Fig. (10) is drawn for $\alpha(w,\rho) = \frac{20-exp(w\rho)}{600}$ and $\beta(w,\rho) = 0.8+0.01w^2\rho^2$. Figs. (9)-(10) show that the diffusion process becomes slow in presence of source term ($\lambda = 1$) as compared to the CS ($\lambda = 0$) and sink term ($\lambda = -1$).

7. Conclusions

The goal of this paper is to present a numerical approach for solving nonlinear variable-order ARDE by using Vieta-Fibonacci operational matrix method and collocation technique. It is analytically found that the obtained approximate solution converges rapidly to exact solution with the convergence order $O\left(\frac{1}{k}\right)$ as degree of approximation (k) increases and the accuracy of the scheme is verified by two examples. Therefore, this study shows that the proposed scheme is sufficiently accurate and effective to solve variable-order non-linear differential equations. The effect of various parameters of the proposed model on the concentration profiles are also analyzed, and it is found that the diffusion process becomes fast for conservative system than the non-conservative system, the presence of advection term in the equation results faster diffusion process, the diffusion process enhances as the value of τ grows and variable-order $\beta(w,\rho)$ and $\gamma(w,\rho)$ are more effective on the diffusion process than the $\alpha(w,\rho)$. Finally, it is our believe that the researchers who are working on non-linear diffusion equations will be benefited by this contribution.

Funding

No Funding.

Author Statement

Rashmi Sharma: Conceptualization, Methodology, Writing-Original draft preparation, Software, Supervision. Rajeev: Conceptualization, Methodology, Software, Supervision. All the authors read and approved the final manuscript.

Competing interests

The authors declare that there is no conflict of interest regarding the publication of this manuscript.

Availability of data and materials:

The authors declare that all the data can be accessed in our manuscript in the numerical simulation section.

References

[1] Jacob Bear and Arnold Verruijt. *Modeling groundwater flow and pollution*, volume 2. Springer Science & Business Media, 2012.

[2] JJ Fried. Groundwater pollution mathematical modelling: improvement or stagnation? In *Studies in Environmental Science*, volume 17, pages 807–822. Elsevier, 1981.

[3] José Francisco Gómez-Aguilar, Margarita Miranda-Hernández, MG López-López, Victor Manuel Alvarado-Martínez, and Dumitru Baleanu. Modeling and simulation of the fractional space-time diffusion equation. *Communications in Nonlinear Science and Numerical Simulation*, 30(1-3):115–127, 2016.

[4] Igor Podlubny. *Fractional differential equations: an introduction to fractional derivatives, fractional differential equations, to methods of their solution and some of their applications*. Elsevier, 1998.

[5] Walter G Glöckle and Theo F Nonnenmacher. A fractional calculus approach to self-similar protein dynamics. *Biophysical Journal*, 68(1):46–53, 1995.

[6] Özkan Güner and Ahmet Bekir. Exact solutions of some fractional differential equations arising in mathematical biology. *International Journal of Biomathematics*, 8(01):1550003, 2015.

[7] Kushal Dhar Dwivedi and Rajeev. Numerical solution of fractional order advection reaction diffusion equation with fibonacci neural network. *Neural Processing Letters*, 53(4):2687–2699, 2021.

[8] Anup Singh, Subir Das, Siew Hui Ong, and Hossein Jafari. Numerical solution of nonlinear reaction–advection–diffusion equation. *Journal of Computational and Nonlinear Dynamics*, 14(4), 2019.

[9] Anup Singh and Subir Das. Study and analysis of spatial-time nonlinear fractional-order reaction-advection-diffusion equation. *Journal of Porous Media*, 22(7):787–798, 2019.

[10] Manpal Singh, S Das, Rajeev, and Siew Hui Ong. Novel operational matrix method for the numerical solution of nonlinear reaction–advection–diffusion equation of fractional order. *Computational and Applied Mathematics*, 41(7):1–18, 2022.

[11] Fawang Liu, Pinghui Zhuang, Vo Anh, Ian Turner, and Kevin Burrage. Stability and convergence of the difference methods for the space–time fractional advection–diffusion equation. *Applied Mathematics and Computation*, 191(1):12–20, 2007.

[12] Prashant Pandey, Sachin Kumar, JF Gómez-Aguilar, and Dumitru Baleanu. An efficient technique for solving the space-time fractional reaction-diffusion equation in porous media. *Chinese Journal of Physics*, 68:483–492, 2020.

[13] Taghreed A Assiri. Time-space variable-order fractional nonlinear system of thermoelasticity: numerical treatment. *Advances in Difference Equations*, 2020(1):1–27, 2020.

[14] Abiola D Obembe, M Enamul Hossain, and Sidqi A Abu-Khamsin. Variable-order derivative time fractional diffusion model for heterogeneous porous media. *Journal of Petroleum Science and Engineering*, 152:391–405, 2017.

[15] MH Heydari, Z Avazzadeh, and A Atangana. Orthonormal shifted discrete legendre polynomials for solving a coupled system of nonlinear variable-order time fractional reaction-advection-diffusion equations. *Applied Numerical Mathematics*, 161:425–436, 2021.

[16] Pinghui Zhuang, Fawang Liu, Vo Anh, and Ian Turner. Numerical methods for the variable-order fractional advection-diffusion equation with a nonlinear source term. *SIAM Journal on Numerical Analysis*, 47(3):1760–1781, 2009.

[17] Ruige Chen, Fawang Liu, and Vo Anh. Numerical methods and analysis for a multi-term time–space variable-order fractional advection–diffusion equations and applications. *Journal of Computational and Applied Mathematics*, 352:437–452, 2019.

[18] Farnaz Kheirkhah, Mojtaba Hajipour, and Dumitru Baleanu. The performance of a numerical scheme on the variable-order time-fractional advection-reaction-subdiffusion equations. *Applied Numerical Mathematics*, 178:25–40, 2022.

[19] Kolade M Owolabi. Numerical simulation of fractional-order reaction–diffusion equations with the riesz and caputo derivatives. *Neural Computing and Applications*, 32(8):4093–4104, 2020.

[20] Praveen Agarwal, AA El-Sayed, and Jessada Tariboon. Vieta–fibonacci operational matrices for spectral solutions of variable-order fractional integro-differential equations. *Journal of Computational and Applied Mathematics*, 382:113063, 2021.

[21] Mohammad Hossein Heydari and Zakieh Avazzadeh. Legendre wavelets optimization method for variable-order fractional poisson equation. *Chaos, Solitons & Fractals*, 112:180–190, 2018.

[22] Sachin Kumar, Prashant Pandey, and Subir Das. Gegenbauer wavelet operational matrix method for solving variable-order non-linear reaction–diffusion and galilei invariant advection–diffusion equations. *Computational and Applied Mathematics*, 38(4):1–22, 2019.

[23] Mojtaba Hajipour, Amin Jajarmi, Dumitru Baleanu, and HongGuang Sun. On an accurate discretization of a variable-order fractional reaction-diffusion equation. *Communications in Nonlinear Science and Numerical Simulation*, 69:119–133, 2019.

[24] MH Heydari and A Atangana. An optimization method based on the generalized lucas polynomials for variable-order space-time fractional mobile-immobile advection-dispersion equation involving derivatives with non-singular kernels. *Chaos, Solitons & Fractals*, 132:109588, 2020.

[25] Mohammad Hossein Heydari and Zakieh Avazzadeh. Numerical study of non-singular variable-order time fractional coupled burgers equations by using the hahn polynomials. *Engineering with Computers*, 38:101–110, 2020.

[26] Rashmi Sharma, Rajeev. An operational matrix approach to solve a 2d variable-order reaction advection diffusion equation with vieta–fibonacci polynomials. *Special Topics & Reviews in Porous Media: An International Journal*, 14(5), 2023.

[27] Rashmi Sharma, Rajeev. A numerical approach to solve 2d fractional rade of variable-order with vieta–lucas polynomials. *Chinese Journal of Physics*, 86:433–446, 2023.

[28] Dan-Dan Dai, Ting-Ting Ban, Yu-Lan Wang, and Wei Zhang. The piecewise reproducing kernel method for the time variable fractional order advection-reaction-diffusion equations. *Thermal Science*, 25(2B):1261–1268, 2021.

[29] M Hosseininia, MH Heydari, Z Avazzadeh, and FM Maalek Ghaini. A hybrid method based on the orthogonal bernoulli polynomials and radial basis functions for variable order fractional reaction-advection-diffusion equation. *Engineering Analysis with Boundary Elements*, 127:18–28, 2021.

[30] Hai-Dong Qu, Xuan Liu, Xin Lu, Mati ur Rahman, and Zi-Hang She. Neural network method for solving nonlinear fractional advection-diffusion equation with spatiotemporal variable-order. *Chaos, Solitons & Fractals*, 156:111856, 2022.

[31] Kushal Dhar Dwivedi, Rajeev, Subir Das, and Dumitru Baleanu. Numerical solution of nonlinear space–time fractional-order advection–reaction–diffusion equation. *Journal of Computational and Nonlinear Dynamics*, 15(6):061005, 2020.

DEPARTMENT OF MATHEMATICAL SCIENCES, INDIAN INSTITUTE OF TECHNOLOGY, VARANASI, 221005, UTTAR PRADESH, INDIA

E-mail address: rashmi.sharma.rs.mat18@itbhu.ac.in (R. Sharma)

E-mail address: rajeev.apm@iitbhu.ac.in (Rajeev)